ARL-TR-9268 ● AUG 2021

Validation of an Exploding-Wire Circuit Model

by Paul R Berning and W Casey Uhlig

NOTICES

Disclaimers

The findings in this report are not to be construed as an official Department of the Army position unless so designated by other authorized documents.

Citation of manufacturer's or trade names does not constitute an official endorsement or approval of the use thereof.

Destroy this report when it is no longer needed. Do not return it to the originator.

ARL-TR-9268 ● AUG 2021

Validation of an Exploding-Wire Circuit Model

Paul R Berning and W Casey Uhlig
Weapons and Materials Research Directorate,
DEVCOM Army Research Laboratory

REPORT DOCUMENTATION PAGE

Form Approved
OMB No. 0704-0188

1. REPORT DATE *(DD-MM-YYYY)*	2. REPORT TYPE	3. DATES COVERED (From - To)
August 2021	Technical Report	1 October 2020–30 July 2021

4. TITLE AND SUBTITLE
Validation of an Exploding-Wire Circuit Model

5a. CONTRACT NUMBER

5b. GRANT NUMBER

5c. PROGRAM ELEMENT NUMBER

6. AUTHOR(S)
Paul R Berning and W Casey Uhlig

5d. PROJECT NUMBER

5e. TASK NUMBER

5f. WORK UNIT NUMBER

7. PERFORMING ORGANIZATION NAME(S) AND ADDRESS(ES)
DEVCOM Army Research Laboratory
ATTN: FCDD-RLW-TA
Aberdeen Proving Ground, MD 21005

8. PERFORMING ORGANIZATION REPORT NUMBER
ARL-TR-9268

9. SPONSORING/MONITORING AGENCY NAME(S) AND ADDRESS(ES)

10. SPONSOR/MONITOR'S ACRONYM(S)

11. SPONSOR/MONITOR'S REPORT NUMBER(S)

12. DISTRIBUTION/AVAILABILITY STATEMENT
Approved for public release: distribution unlimited.

13. SUPPLEMENTARY NOTES

14. ABSTRACT
A series of exploding-wire experiments involving copper, aluminum, tungsten, and titanium wires was performed as part of a program whose ultimate aim is to validate the multiphysics code ALEGRA. This work describes the results of these exploding-wire experiments and reports on the efficacy of a circuit model developed to predict key features in the data such as peak current and the timing of phase changes.

15. SUBJECT TERMS
exploding wire, circuit model, pulsed power, magnetic instabilities, thermophysical properties

16. SECURITY CLASSIFICATION OF:			17. LIMITATION OF ABSTRACT	18. NUMBER OF PAGES	19a. NAME OF RESPONSIBLE PERSON
a. REPORT	b. ABSTRACT	c. THIS PAGE			Paul R Berning
Unclassified	Unclassified	Unclassified	UU	45	19b. TELEPHONE NUMBER (Include area code) (410) 278-4509

Contents

List of Figures

List of Tables

1. Introduction

As pointed out in Berning and Coppinger,[1] an exploding-wire experiment can include many complicated effects, to the point where faithfully simulating the events requires a complex multiphysics code such as ALEGRA.[2,3] The experiments described here are part of a program whose ultimate goal is to conduct experiments that can be used to judge how well ALEGRA handles all the complicating factors that can arise in pulsed-power experiments. This report, however, has the more modest goal of reporting on the results of a series of exploding-wire experiments and to report on the performance of the exploding-wire circuit model described in Berning and Coppinger. As the purpose of the circuit model was limited to making predictions about key features such as the peak current achieved and the timing of phase changes, it did not account for all the relevant physics. It would be difficult or impossible to include complicated features such as skin-depth effects and magneto-hydrodynamic (MHD) instabilities[1] in a circuit model in any event. In this report, we describe the results of a number of exploding-wire experiments involving wires made of copper (Cu), aluminum (Al), tungsten (W), and titanium (Ti) and demonstrate where the circuit model works well and where it does not.

At its core, the circuit model is a series *LRC* circuit model (where *L* indicates lumped inductance, *R* indicates lumped resistance, and *C* indicates capacitance). Kirchoff's law provides the governing differential equation:

$$\frac{Q}{C} + R\frac{dQ}{dt} + \frac{d}{dt}\left(L\frac{dQ}{dt}\right) = 0 \qquad (1)$$

where Q is the charge on the capacitor and the current in the loop is defined as $I = -dQ/dt$. In an exploding-wire experiment, C is naturally constant, R changes in time in response to ohmic heating and thermal expansion, and L changes in time due to expansion, particularly after vaporization occurs.

The circuit model in question uses published values of resistivity and heat capacity to track the temperature rise through the solid and liquid phases, but not the vapor phase, as published values of metal vapor resistivity were not available. Since the model is not valid past the point where vaporization occurs, and most of the physical expansion occurs in the vapor/plasma phase, it was decided to simply assume that L remains constant during the times where the model is valid. This is equivalent to assuming that the wire retains its initial geometry at all times, hence it ignores the effects of thermal expansion. It also ignores skin-depth effects.

Beyond the predicted boiling point, the model assumes the temperature dependence of the resistivity of the liquid phase still applies and that the geometry remains unchanged. While decidedly unphysical, this was done simply to supply something to compare with in the vapor-phase portion of the event.

Despite the fact that the model does not accommodate such things as skin-depth effects and MHD instabilities, the model performed fairly well during periods where vaporization was not widespread. In some cases, the analysis was complicated by unexpected behavior associated with certain aspects of the experimental setup. These irregularities are also discussed.

2. Exploding-Wire Experiments

2.1 Physical Layout

The pure metal wires used in these experiments were supplied by ESPI Metals (Ashland, Oregon) in the form of straight rod. They consisted of "4N" Cu (i.e., 99.99% copper), "4N" Al, "3N8" W (i.e., 99.98% tungsten), and "4N" Ti. All had diameters of 1.590 mm.

The experimental arrangement uses a power supply similar to that used in Zellner et al.,[4] in that it used three ICAR Bioenergy Model D 65-B 62.5-2000 capacitors (ICAR S.p.A, Monza, Italy), nominally representing 38 kJ of stored energy at 20 kV. The actual power supply used in these experiments was an upgraded version that included a relatively low-inductance built-in spark-gap switch.[5] The total capacitance of the capacitor bank was measured to be 189 μF. The preset initial voltages ("V_0") on the bank should be accurate to within ±1%.

Figure 1 contains both a drawing and a photograph of the wire mounting provisions used in these experiments. As can be seen, the Al mounting structure was rigidly mounted to the power supply. This was done to enforce a constant geometry and thus maintain a constant total inductance. Current was fed to one end of the wire by two Al bars, one above the wire and one below, to balance the $J \times B$ forces on the wire. The bars were spaced off the wire by about 65 mm to allow for unimpeded high-speed video and flash X-ray coverage. They were attached to a rectangular end plate large enough to allow for some current spreading so the current feed would appear to be at least quasi-axisymmetric.

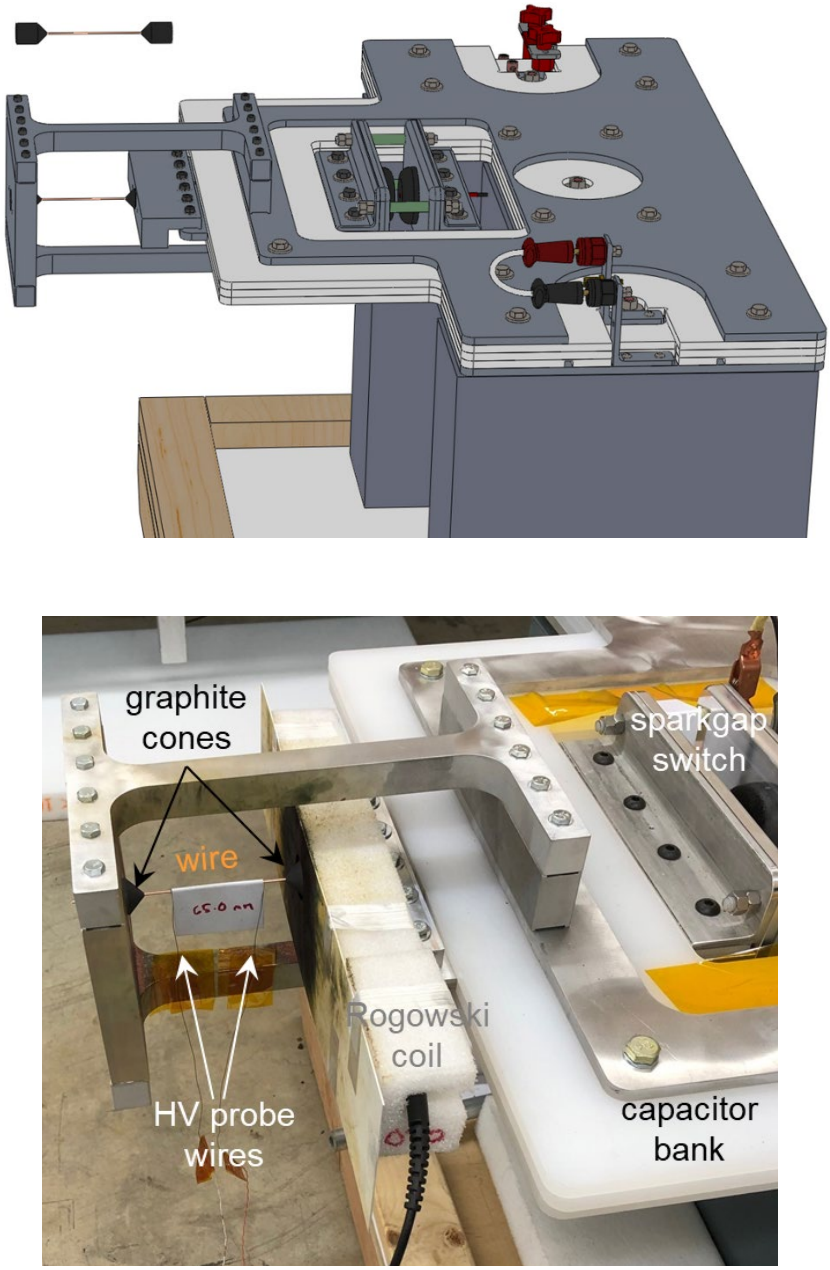

Fig. 1 Experimental setup

One unusual feature of this setup was that the ends of the wires were encased in conical graphite buffer plugs (highlighted in the drawing in Fig. 1, top left). These were included to ameliorate the problem of the ends of the wire blowing off early due to the MHD instabilities that inevitably set up at those locations. In Zellner et al.[4] it was found that the rapidly expanding vapor clouds arising from the exploding ends would quickly encompass the entire volume under study, complicating the analysis. Modeling with ALEGRA indicated that the inclusion of the 25-mm-diameter graphite plugs would greatly slow down this process[6] due to the large skin

depth seen in graphite. At the frequencies used in these experiments, most of the current flows within 1 mm of the surface of any of the metal components. In graphite, the skin depth is closer to 25 mm, allowing the current to spread throughout the volume of the graphite buffer plug and distribute the current along some length of the enclosed portion of wire. This avoids the abrupt turn in current flow that leads to an MHD instability when metal end connections are used (even when the metal is heavily tapered[4]). The graphite used was supplied by McMaster-Carr (Elmhurst, Illinois). Its density was measured to be 1.76 g/cm^3, and its room temperature resistivity was measured to be 11.78 μΩ-m.

Difficulties associated with rapidly expanding vapor clouds in exploding-wire experiments are often handled by immersing the wire in water[3,7] (and thus confining the vapor) or performing the experiment under high-pressure conditions[8] (to suppress boiling). As we wish to see if ALEGRA can recreate effects associated with the expanding clouds of metal vapor in open air, these strategies were not used here.

For the purposes of this report, when "the wire" is referenced, it refers to the exposed length of the wire only, which was roughly 101 mm long in all cases. For the most part, the portions of the wire within the graphite plugs were considered part of the mounting provisions and were ignored in the analysis. This proved problematic in the case of Ti, however, because the mounting provisions appeared to add a considerable amount of parasitic resistance to the circuit for reasons that are not entirely clear.

2.2 Diagnostics

High-speed video was used in most of the experiments to observe the response of the wire to the electrical pulse. In all cases, the wire itself supplied the illumination, so the images primarily highlight the times when very hot metal or metal vapor is present. The camera used was a Shimadzu model HPV-X2 set to record 128 images at a frame rate of 2 MHz, an exposure time of 200 ns, and a resolution of 400 × 250 pixels. A neutral density filter (value 3.9) was used in all experiments to attenuate the light level. Various aperture settings were used as well, tailored to the particular situation.

The electrical diagnostics included a Rogowski coil that measured the time rate of change of the current (dI/dt). Current as a function of time was obtained via numerical integration of the Rogowski data. The Rogowski coil used was a US Army Combat Capabilities Development Command Army Research Laboratory design. The calibration uncertainty associated with this design is approximately 3%; however, most of that comes from residual position sensitivity. When the

conductor is firmly held at the center of the coil (as was done in these experiments), the uncertainty is closer to 1%.

An additional uncertainty derives from the numerical integration process. Due to small voltage biases in the oscilloscope, the integrated Rogowski signal acquires a roughly linear background, which must be subtracted to obtain the proper current versus time signal. This procedure is very accurate when the voltage bias remains constant over the duration of the pulse; however, this is not always the case. In each data set, a linear background is subtracted such that the current returns to zero at the end of the pulse, but if the oscilloscope bias varied during the pulse, small errors are introduced into the final result. As the quality of the oscilloscope bias varies from one experiment to the next, it is difficult to apply a single level of uncertainty to the background subtraction procedure; however, it seldom affects the peak current measurement by more than 1% or 2%. The high level of repeatability seen in the experiments described in this work is a testament to that fact. Note the oscilloscope biases are typically in the millivolt range and thus have virtually no effect on the dI/dt measurements themselves.

In virtually all the experiments described in this report, the voltage difference between the two ends of the Al mounting fixture was recorded as a function of time. In most but not all of the experiments, the voltage difference across an approximately 65-mm-long section of the wire was also recorded. The latter measurements were made to bypass the influence of the exploding wire ends. The four high-voltage probes used were all Northstar High Voltage Model PVM-2 voltage probes, which have a listed uncertainty of less than 1.5% between 200 Hz and 500 MHz (Northstar High Voltage, Bainbridge Island, Washington).

Contact to the ends of the 65-mm section was made by hooking two pieces of 32-AWG (i.e., 0.2-mm-diameter) bent copper wire over the wire under test. As seen in the high-speed video images later in this report, even this minor addition perturbs the expanding metal to the point where it eventually seeds an MHD instability, causing the metal at those locations to vaporize early just as the ends do. This would appear to have little effect on the electrical measurements, however, as the electrical data obtained in experiments where the 32-AWG wires were used are in excellent agreement with the data obtained in nearly identical experiments where they were not used.

As the graphite plugs were slip-fit into the Al mounting structure, the length of exposed wire varied slightly from test to test. Images recorded by the high-speed video camera were used to accurately measure the length of the exposed wire and distance between the 32-AWG wire hooks. As demonstrated in Fig. 2, the camera images were calibrated by inserting a 1-inch-wide machinist's rule into the

mounting holes for the graphite plugs (which were slightly wider than 1 inch). The locations of roughly 25 marks on the rule, in terms of pixels, were noted and a linear fit was performed. Uncertainty in the length of the wire was on the order of ±1 pixel, or ±0.38 mm. The uncertainty in the distance between the 32-AWG wire hooks is probably closer to ±2 pixels, as it was sometimes difficult to identify the exact contact points.

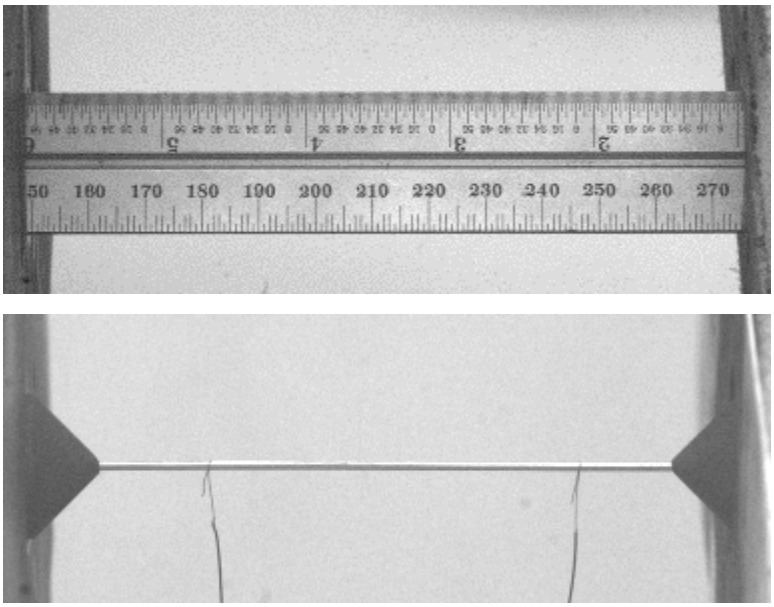

Fig. 2 Length measurement

2.3 Analysis

As pointed out in Berning and Coppinger,[1] some of the input parameters for the circuit model must be derived from the data, in particular the parasitic inductance in the circuit (i.e., all of the inductance in the circuit not accounted for in the exposed length of wire). Determining the total inductance of the circuit is best done by examining the behavior near $t = 0$, when $I = 0$. At that point in time, Kirchoff's law simplifies to

$$V_0 = -L_{tot}\frac{dI}{dt}\Big|_{t=0} \tag{2}$$

Hence, the total inductance of the circuit L_{tot} can be determined if the initial voltage on the bank (V_0) is known and the initial risetime ($dI/dt|_{t=0}$) is known. The parasitic inductance can then be determined by subtracting the inductance of the wire, calculated using a standard formula.[1,9] Similarly, Eq. 2 can be used to determine the initial inductance of the wire mount plus wire system if "V_0" is replaced by the initial voltage difference measured across the mount.

In performing this operation over many experiments, a difficulty became apparent: The apparent total inductance at $t = 0$ varied more than it should have based on the measurement uncertainties in V_0 and dI/dt. In particular, the values derived in the higher-resistance cases (involving W and Ti) were noticeably higher than the average value seen in other experiments. It is hypothesized that the paths the current took within the graphite plugs were somehow more constrained in those situations, thus adding to the overall inductance. It was noted that the fit between the wire and graphite was a bit looser in those cases. This may also have affected the geometry of the current flow within the graphite.

Despite this oddity, using the average value of the parasitic inductances determined over the course of 21 experiments proved to be perfectly acceptable. In all cases, that assumption yielded reasonable agreement with the data where agreement would be expected (i.e., below the boiling point). In all of the following simulations, the parasitic inductance was assumed to be $L_p = 224.8$ nH. The portion of that associated with the wire mounting structure was assumed to be $L_m = 30.6$ nH.

The variable inductance issue may be related to a discrepancy seen in the Ti cases, where a large parasitic resistance had to be attributed to the wire mounting system to explain the data. This effect was not seen in experiments involving Cu, Al, or W. In those cases, it was found that adding in a small amount of parasitic resistance would improve agreement slightly, but the amount needed ($\sim R_p = 0$ to $R_p = 2.5$ mΩ) was small and varied between experiments. Zero typically worked best in high-energy experiments, and 2.5 typically worked best in low-energy experiments. Ultimately, it was decided that the effects associated with such small amounts of parasitic resistance were too small for this relatively low-fidelity model to accurately resolve and thus the numbers derived were largely meaningless (i.e., assuming that $R_p = 0$ in all cases was an acceptable assumption). Similarly, while sometimes attributing a portion of the total parasitic resistance to the wire mounting system improved the voltage prediction slightly, those numbers were also likely meaningless.

The Ti cases proved an exception to this rule, however, as the current traces measured in those cases could only be explained if the total parasitic resistance was in excess of 10 mΩ, and the voltage traces measured could only be explained if much of that parasitic resistance was found in the wire mounting system. While Ti is a relatively poor conductor, so also is W, and the effect was not seen in those cases. The slightly looser fit of the wires may have played a role, though an attempt to rectify that failed to make a difference.

2.4 Energies Used

The levels of stored energy in the capacitor bank ($E = \frac{1}{2}CV_0^2$) used in these experiments were chosen somewhat arbitrarily. Three energy levels were used for each metal. In the Cu, Al, and W cases, the energy levels were chosen to be roughly 47%, 82%, and 128% of the energy needed to fully vaporize a mass of metal equivalent to that contained in a 101-mm-long, 1.590-mm-diameter wire. In the case of the Ti experiments, the energy levels were chosen to be roughly 18%, 44%, and 81% of the total energy needed to vaporize the mass of metal in a 101-mm-long, 1.590-mm-diameter Ti wire. The lowest energy Ti experiment was performed to test the circuit model in the low-temperature regime, where in theory it should perform best. The specific levels of energy used are listed in the Appendix. The levels of energy needed to achieve certain waypoints in the temperature curves and/or phase diagrams are listed in Table 1.

Table 1 Estimated energies, in kilojoules, required to reach certain waypoints in the temperature curves/phase diagrams of the wires tested

Waypoints	Cu	Al	W	Ti
Melting point	0.84	0.36	2.36	1.05
Fully melted	1.21	0.58	3.52	1.31
Boiling point	2.59	1.76	6.00	2.82
Fully vaporized	11.08	7.66	23.87	10.56

3. Experimental Results

3.1 Cu Wire Experiments

"Shot #5" was an experiment in which a copper wire was used and the capacitor bank was initially charged to 7.5 kV (representing 5.3 kJ of stored energy). The length of the exposed portion of wire was determined to be 101.3 mm, and the distance between the 32-AWG probe wires was 65.5 mm. Figure 3 contains a plot of the current versus time data compared with results of two simulations, one where the total parasitic resistance (R_p) is assumed to be 0 mΩ and one assumed to be 2 mΩ. Note that while agreement is better in the R_p = 2 mΩ case, the effects are largely cosmetic. Agreement is excellent up to the t = 55-μs point.

The model predicts that if heating were uniform, the melting point temperature would be achieved at 28.3 μs, the wire would be fully melted at 32.9 μs, and the boiling point would be reached at 39.8 us. The theoretical melting and boiling

points are marked in Fig. 3. The level of energy used in this experiment is insufficient to fully vaporize the wire.

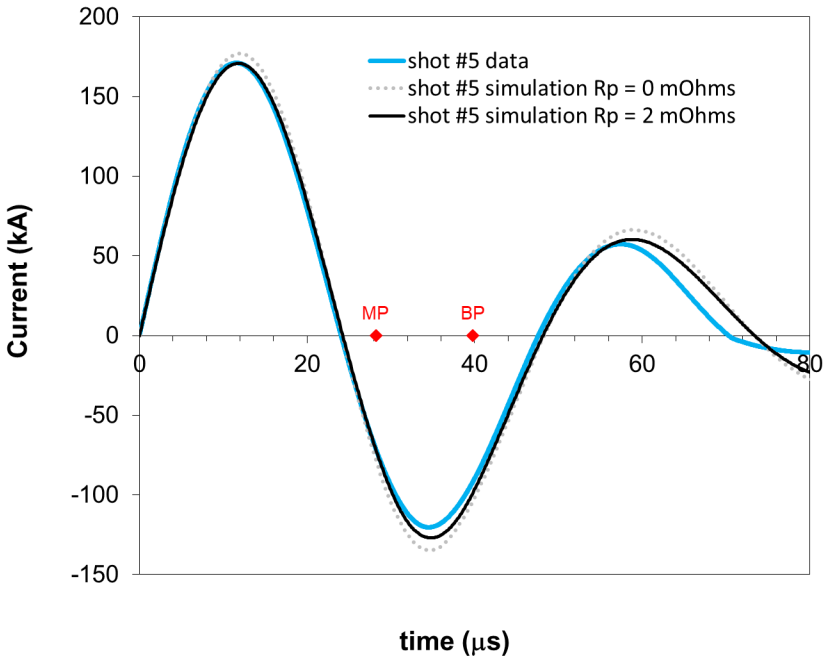

Fig. 3 Shot #5 current data compared with the results of two simulations

Figure 4 contains plots of the voltage data obtained from Shot #5 compared with the results of simulations (wire mount data were smoothed to reduce the effects of noise). Two simulations were run in the case of the voltage across the wire mount, one that assumes that the wire mount itself has resistance $R_m = 0$ mΩ (and $R_p = 0$ mΩ) and one that assumes the wire mount has $R_m = 1.5$ mΩ (and $R_p = 2$ mΩ). Note the difference between the two cases is small. Agreement is good in either case.

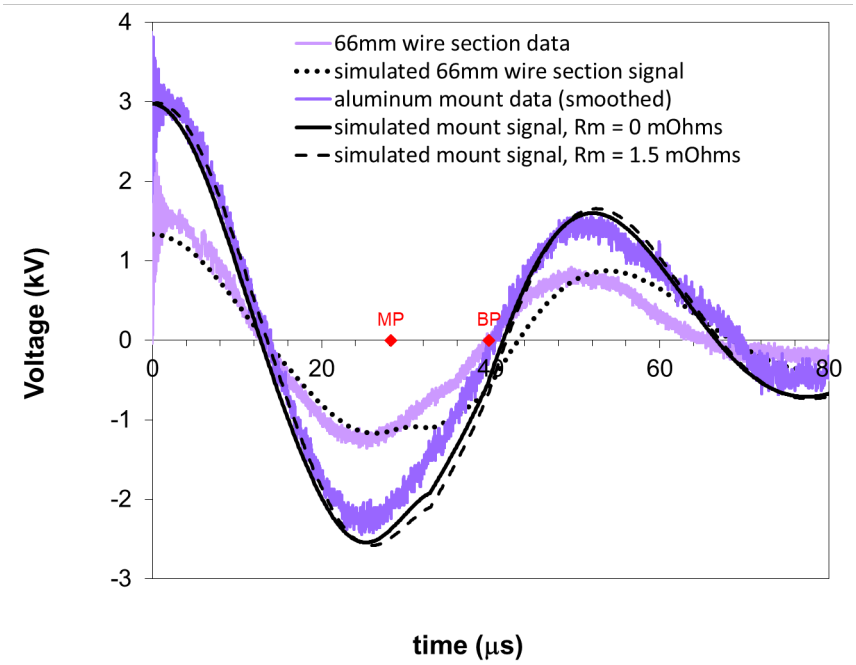

Fig. 4 Shot #5 voltage data compared with the results of simulations

The simulated voltage signal across the 65.5-mm central portion of the wire underestimates the initial voltage and seems to be slightly out of phase with the data. This occurs in virtually all of the experiments reported on here. While it is possible that the model is consistently underestimating the inductance of this portion of wire, it is also possible that the high-voltage probe circuit was affected by stray fields. Uncertainties in the length and diameter of the wires are not enough to explain this discrepancy. Agreement is still reasonable despite this. Note the model predicts significant artifacts associated with phase changes whereas the associated artifacts in the data are more subtle. This is likely due to the model's assumption that the heating is uniform, when in reality, skin-depth effects and instabilities cause some portions of the wire to change phase before other portions do.

Figure 5 contains a frame taken by the high-speed video camera at t = 59.95 μs. In this experiment, clear images are only available for times late in the pulse and beyond, when there is sufficient hot metal vapor present to supply lighting. In Fig. 5 it is evident that instabilities have set up at both ends of the wire and beneath the right high-voltage probe wire. The rest of the copper exhibits a series of kink instabilities, where subtle kinks present in the wire are magnified by magnetic forces (if the wire is bent into a helix, it is referred to as a "screw instability"). In the video frames following this one, the vapor clouds have expanded, the left probe wire has instituted an MHD instability of its own, and the kink instabilities are more pronounced.

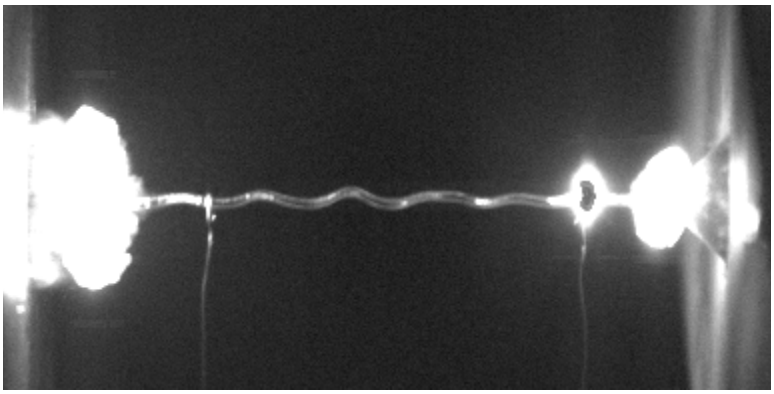

Fig. 5 High-speed video frame from Shot #5

"Shot #6" was an experiment in which a pure copper wire was used and the capacitor bank was initially charged to 10.0 kV (representing 9.45 kJ of energy). The length of the exposed portion of wire was determined to be 101.6 mm, and the distance between the 32-AWG probe wires was 64.1 mm. Figure 6 contains a plot of the current data compared with results of a simulation where it was assumed that $R_p = 1$ mΩ (as before, this yields only a tiny improvement over the $R_p = 0$ mΩ version). Agreement is excellent up to about the 30-μs point. Data taken from two nearly identical experiments ("Shot 8" and "Shot #9") are also plotted, demonstrating the excellent repeatability of these experiments (the traces virtually overlay each other). Since the 32-AWG probe wires were not included in Shots #8 and #9, it would appear that the presence of the 32-AWG probe wires had little effect on the outcome of these experiments.

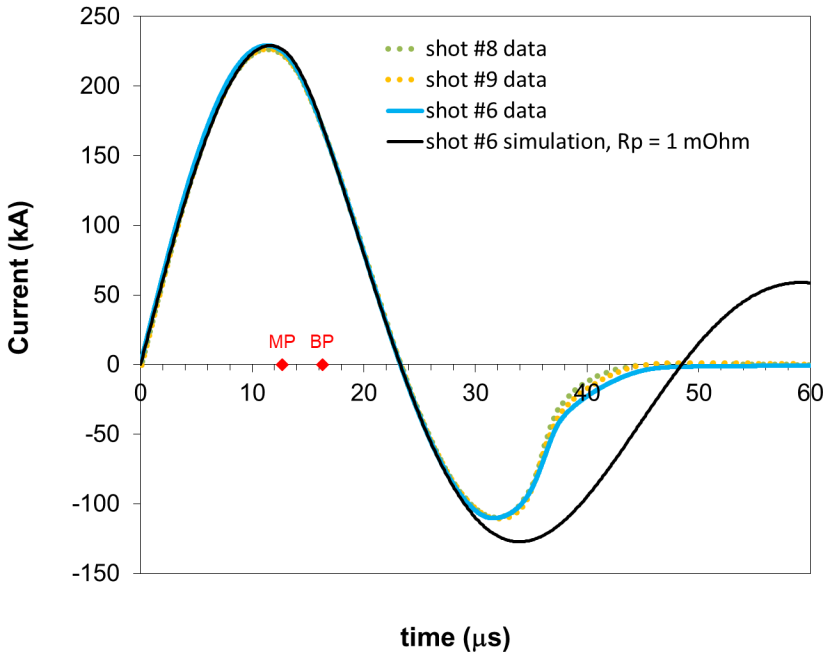

Fig. 6 Shots #6, #8, and #9 current data compared with a simulation

Figure 7 contains plots of the voltage data obtained from Shot #6 compared with the results of a simulation where it was assumed that $R_m = 1$ mΩ (as before, this improves the simulated mount voltage signal only slightly). Here, agreement is good up to around the 30-μs point. While the simulations once again exaggerate the effects of phase changes, they still appear to get the timing right.

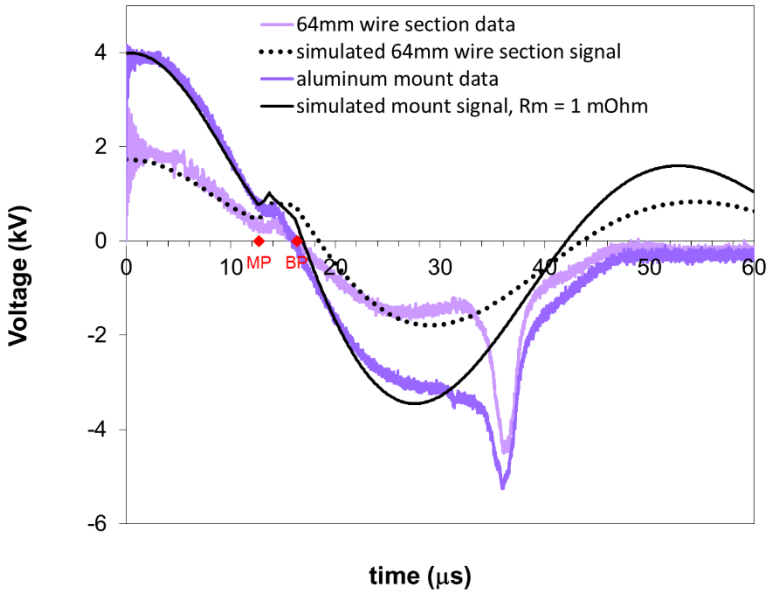

Fig. 7 Shot #6 voltage data compared with simulations

Beyond the 30-μs point, the voltage signals exhibit a "burst" spike associated with a sudden rise in resistance due to vaporization followed quickly by a sudden drop in resistance due to plasma formation.[1] Experience shows that this typically occurs at about the time the individual vapor clouds that form due to localized instabilities expand to the point where they become contiguous across the length of the wire.

In this case, high-speed video showed that kink instabilities similar to those seen in Shot #5 set in early, but they were then rapidly overtaken by thermal or MHD instabilities with a higher spatial frequency. Figure 8 contains a single high-speed video frame taken at t = 35.74 μs, which roughly corresponds to the time the burst spike peaks. At this point, the vapor clouds arising from the various instabilities have expanded to the point where they are contiguous across the wire, as expected. The combination of the various instabilities resulted in nonuniform expansion. The uniformity of the expansion improved as time went on, however.

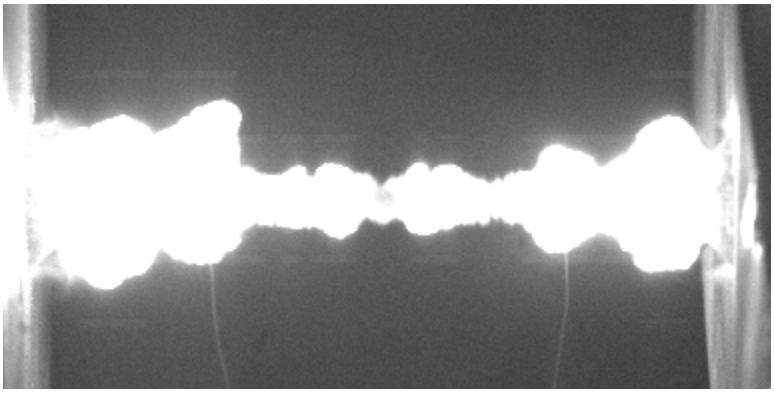

Fig. 8 High-speed video frame from Shot #6

"Shot #7" was an experiment in which a copper wire was used and the capacitor bank was initially charged to 12.5 kV (representing 14.8 kJ of energy). The length of the exposed portion of wire was 101.6 mm, and the distance between the 32-AWG probe wires was 65.2 mm. Figure 9 contains a plot of the current data compared with results of a simulation in which it was assumed that $R_p = 0$ mΩ. As vaporization occurs very quickly in this case, agreement is only good up to about the 16-μs point, roughly where a "burst" event begins. In this case, the resistance increase due to "burst" is sufficient to shut down current flow entirely. Something resembling "restrike"[1] occurs at approximately 54 μs; however, high-speed video indicates this only occurs because the vapor cloud arising from one end of the wire expands to the point where it contacts one of the current return bars and thus shorts the circuit.

Data from "Shot #13", a repeat of Shot #7 where no 32-AWG probe wires were used, are also plotted in Fig. 9. Those data virtually overlay the Shot #7 data.

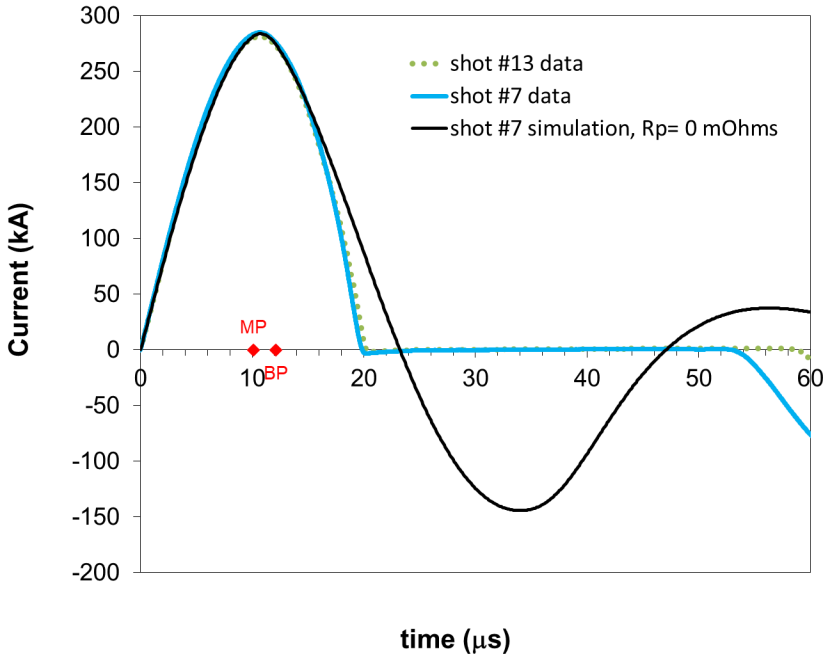

Fig. 9 Shots #7 and #13 current data compared with a simulation

Figure 10 contains plots of the voltage data obtained from Shot #7 compared with the results of a simulation where it was assumed that $R_m = 0$ mΩ. Agreement is good up to around 10 μs, at which point the simulations once again exaggerate the effects of phase changes. After that, the data exhibit a "burst" spike and evidence of current shutdown.

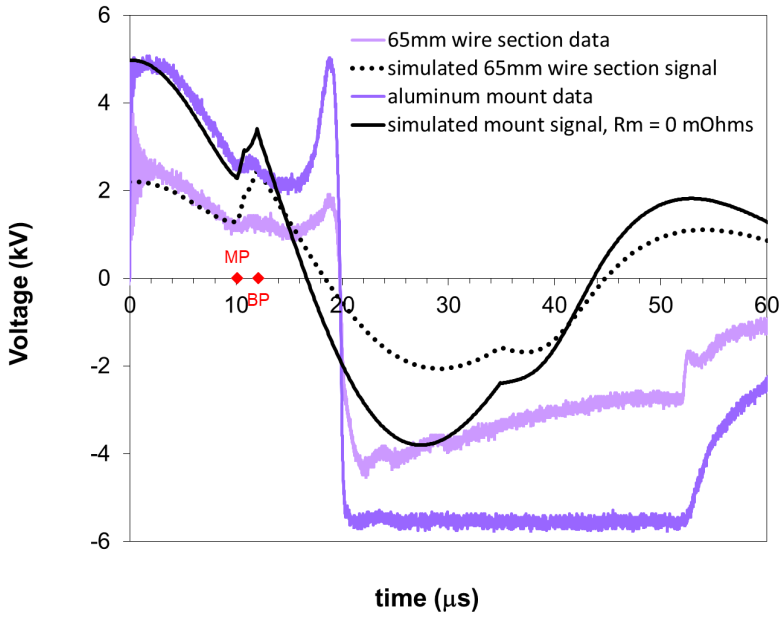

Fig. 10 Shot #7 voltage data compared with simulations

Figure 11 contains a high-speed video frame taken at $t = 18.59$ μs, roughly corresponding to the "burst" peak. Aside from the instabilities at the wire ends and at the locations of the probe wires, the expansion appears to be extremely uniform. There was no hint of any kink instabilities in this case.

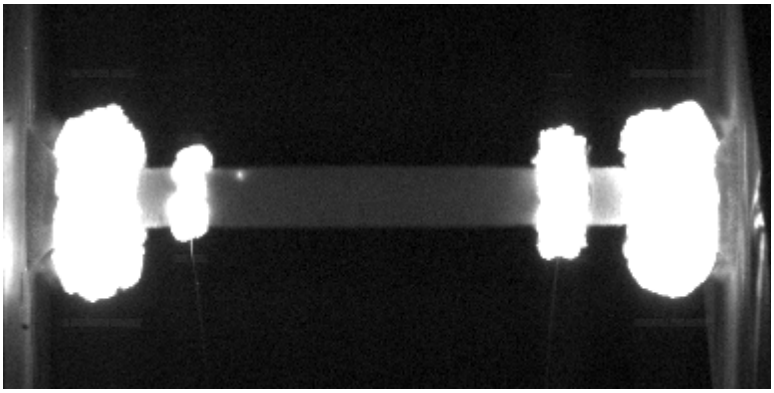

Fig. 11 High-speed video frame from Shot #7

3.2 Al Wire Experiments

"Shot #12" was an experiment in which an Al wire was used and the capacitor bank was initially charged to 6.0 kV (representing 3.4 kJ of energy). The length of the exposed portion of wire was determined to be 102.0 mm, and the distance between the 32-AWG probe wires was 64.8 mm. Figure 12 contains a plot of the current data compared with results of a simulation where it is assumed that $R_p = 2.5$ mΩ. Agreement is good up to about the 30-μs point.

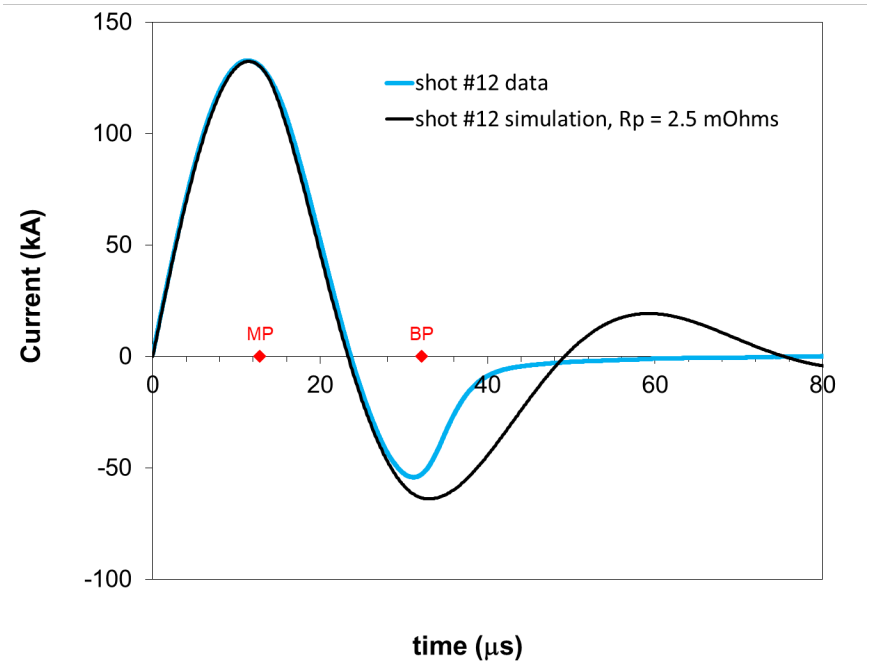

Fig. 12 Shot #12 current data compared with a simulation

Figure 13 contains plots of the voltage data obtained from Shot #12 compared with the results of a simulation where it was assumed that $R_m = 2$ mΩ. Agreement is good up to around $t = 30$ μs, after which a "burst" peak appears in the data. The simulations appear to exaggerate the effects of phase changes once again.

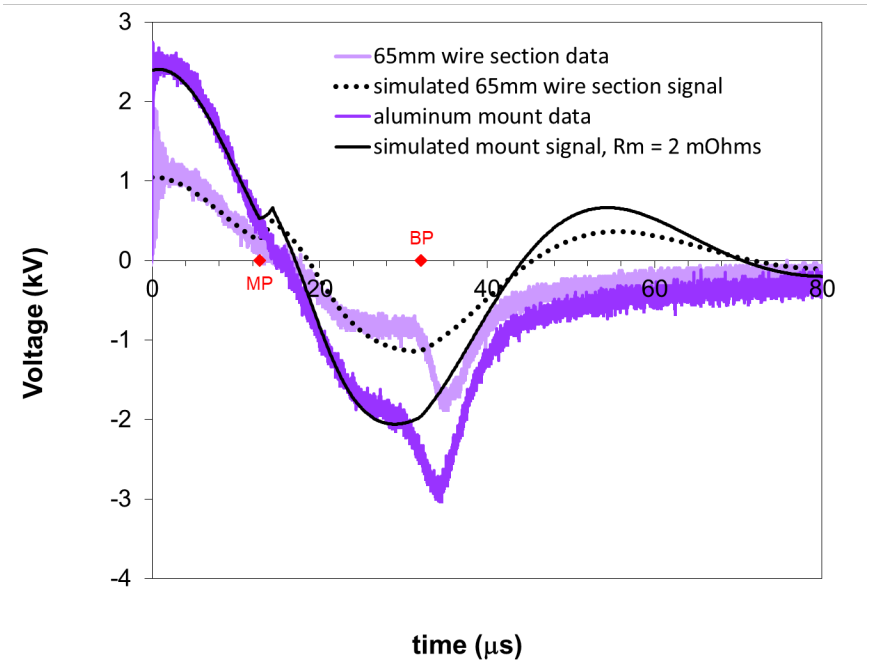

Fig. 13 Shot #12 voltage data compared with simulations

Figure 14 contains a high-speed video frame taken at $t = 34.74$ μs, roughly corresponding to the "burst" peak. No kink instabilities were observed prior to this. Expansion appears to be highly nonuniform with vapor clouds associated with localized instabilities expanding at different rates.

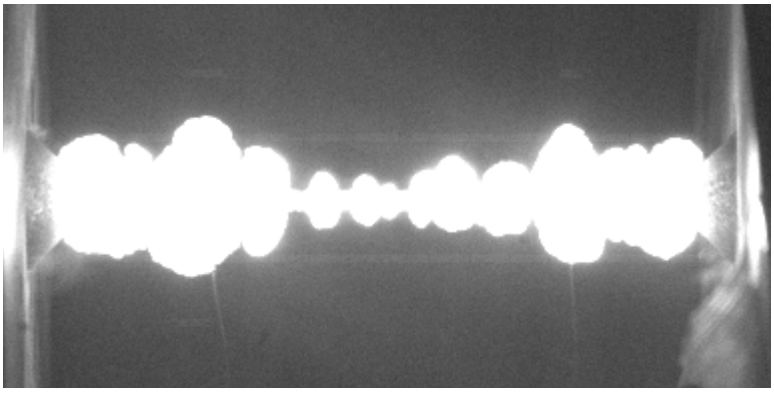

Fig. 14 High-speed video frame from Shot #12

"Shot #11" was an experiment in which an Al wire was used and the capacitor bank was initially charged to 8.0 kV (representing 6.05 kJ of energy). The length of the exposed portion of wire was determined to be 100.1 mm, and the distance between the 32-AWG probe wires was 65.5 mm. Figure 15 contains a plot of the current data compared with results of a simulation where it is assumed that $R_p = 1.5$ mΩ. Agreement is good up to about the 16-μs point.

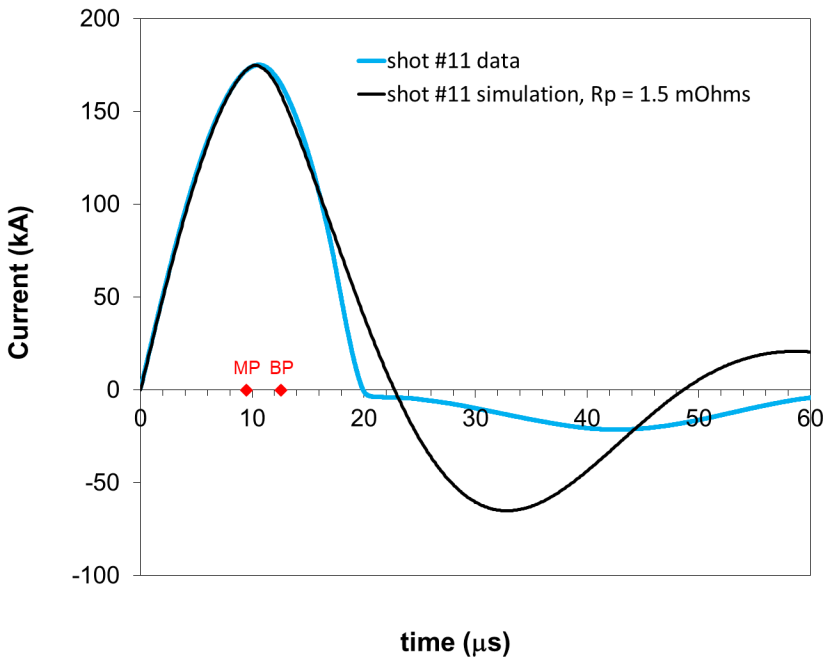

Fig. 15 Shot #11 current data compared with a simulation

Figure 16 contains plots of the voltage data obtained from Shot #11 compared with the results of a simulation where it was assumed that $R_m = 1.5$ mΩ. Agreement is good up to around 16 μs, after which the simulation exaggerates the effects of the phase changes and a "burst" peak appears in the data.

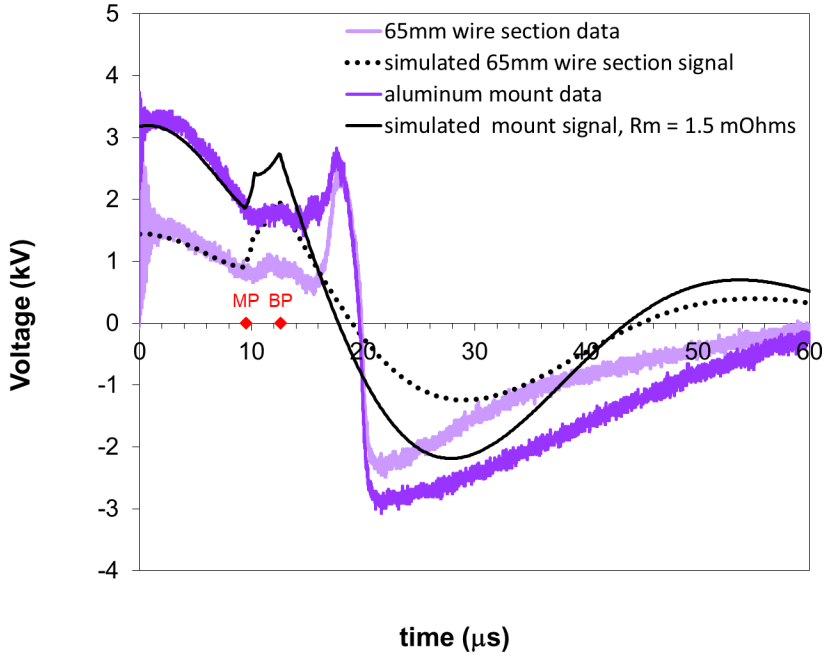

Fig. 16 Shot #11 voltage data compared with simulations

Figure 17 contains a high-speed video frame taken at $t = 18.40$ μs, roughly corresponding to the "burst" peak. Expansion appears to be nonuniform once again.

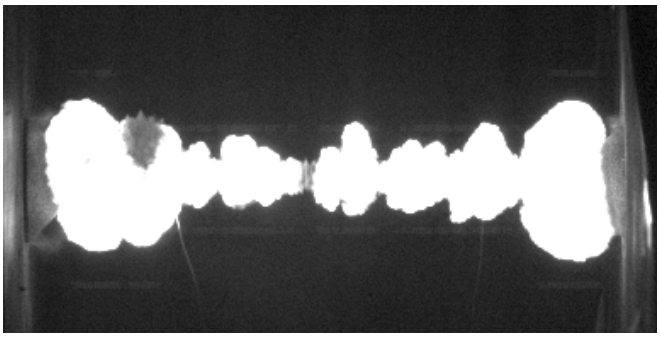

Fig. 17 High-speed video frame from Shot #11

"Shot #10" was an experiment in which an Al wire was used, and the capacitor bank was initially charged to 10.0 kV (representing 9.45 kJ of energy). The length of the exposed portion of wire was determined to be 100.8 mm, and the distance between the 32-AWG probe wires was 65.2 mm. Figure 18 contains a plot of the current data compared with results of a simulation where it is assumed that $R_p = 0$ mΩ. Agreement is good up to about the 12-μs point.

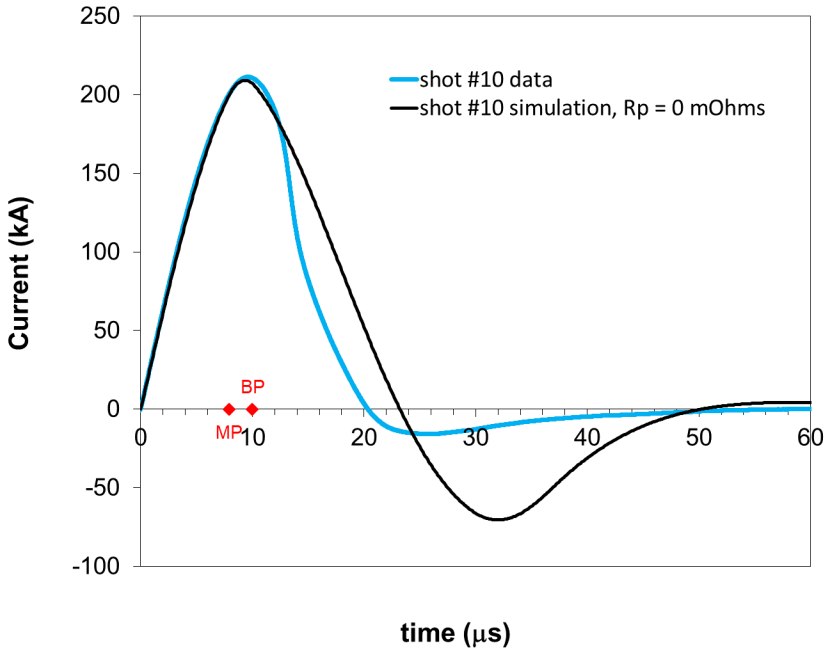

Fig. 18 Shot #10 current data compared with a simulation

Figure 19 contains plots of the voltage data obtained from Shot #10 compared with the results of a simulation where it was assumed that $R_m = 0$ mΩ. Agreement is good up to around 7 μs, after which the simulation exaggerates the effects of the phase changes and a "burst" peak appears in the data.

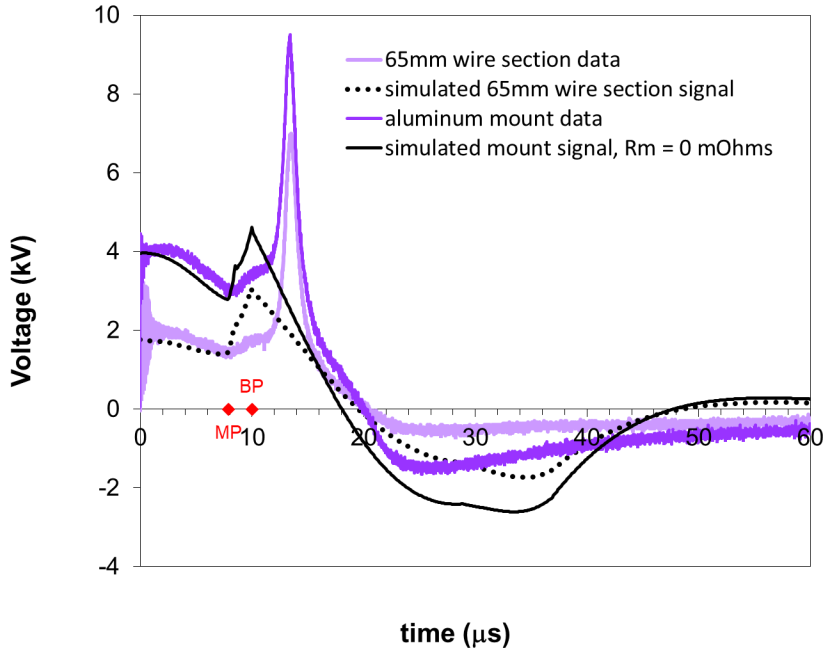

Fig. 19 Shot #10 voltage data compared with simulations

Figure 20 contains a high-speed video frame taken at $t = 13.22$ μs, roughly corresponding to the "burst" peak. Unlike the corresponding high-energy case in Cu, expansion appears to be nonuniform, with vapor clouds associated with localized instabilities expanding at different rates.

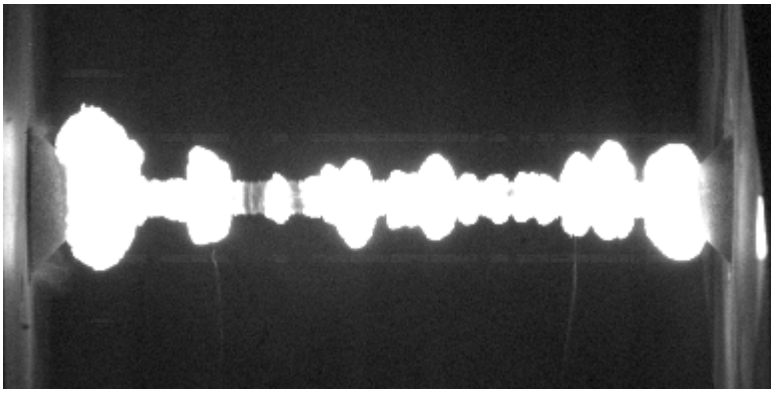

Fig. 20 High-speed video frame from Shot #10

3.3 W Wire Experiments

"Shot #16" was an experiment in which a W wire was used, and the capacitor bank was initially charged to 11.0 kV (representing 11.4 kJ of energy). The length of the exposed portion of wire was determined to be 101.3 mm, and the distance between the 32-AWG probe wires was 64.9 mm. Figure 21 contains a plot of the current data compared with results of a simulation where it is assumed that $R_p = 2.5$ mΩ. Agreement is good up to about the 9-μs point. Unlike previous cases, the model seems to overpredict the resistance in the vapor phase. This suggests that the W vapor is unusually conductive or that it quickly converts to a plasma phase.

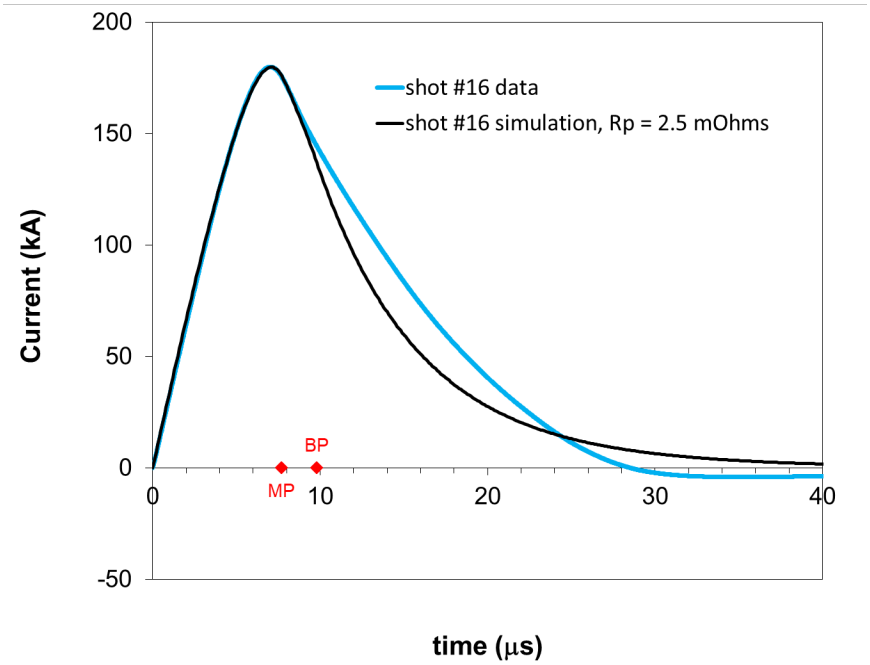

Fig. 21 Shot #16 current data compared with a simulation

Figure 22 contains plots of the voltage data obtained from Shot #16 compared with the results of simulations where it was assumed that $R_m = 2.5$ mΩ and $R_m = 0$ mΩ. Agreement is adequate in the short time that the model is valid. Applying all of the parasitic resistance in the system to the mount improves the mount voltage prediction somewhat. In this case, the model exaggerated the effects of phase changes only slightly. This may mean that the wire was actually heated fairly uniformly (as the model assumes). The relatively good agreement seen in the vapor phase portion is pure coincidence, as the assumptions made by the model in that phase are highly arbitrary. That said, W vapor appears to have a relatively low resistivity compared with the liquid phase. There is no sign of a "burst" peak in the data.

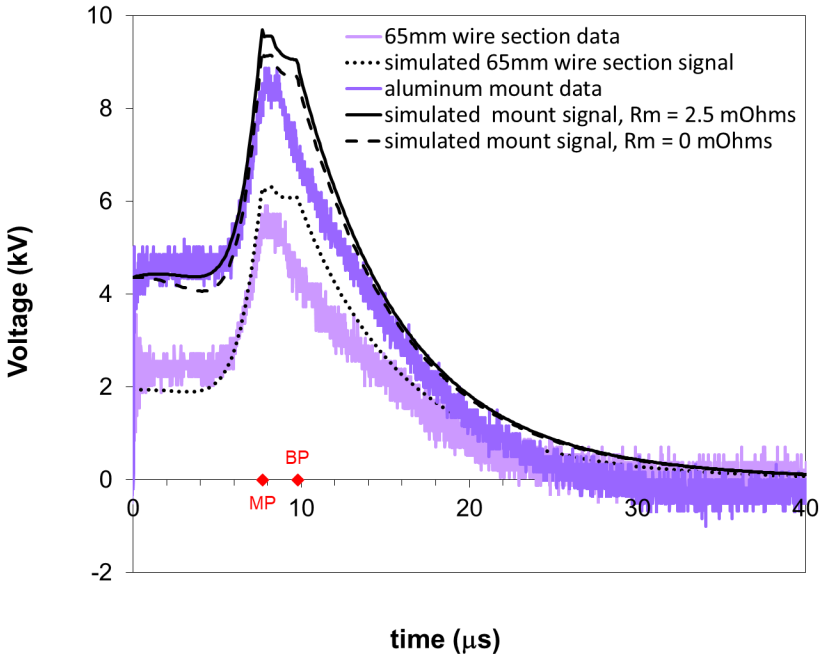

Fig. 22 Shot #16 voltage data compared with simulations

Figure 23 contains two high-speed video frames, the first taken at $t = 7.82$ μs, roughly corresponding to the when the melting point is reached in the simulation, and one taken at $t = 19.82$ μs. Expansion appears to be relatively uniform, with the vapor clouds arising from a large numbers of instabilities expanding at nearly the same rates. Hot gasses can be seen exiting from the edges of the graphite plugs, possibly indicating a loose fit.

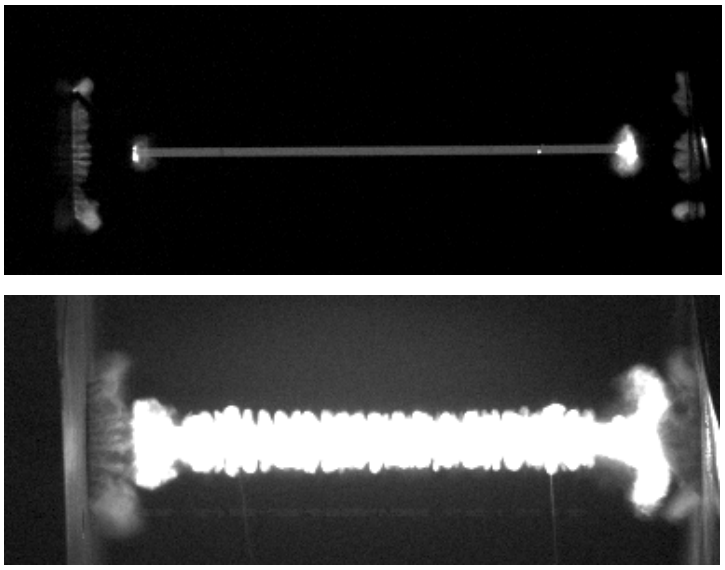

Fig. 23 Two high-speed video frames from Shot #16

"Shot #15" was an experiment in which a W wire was used, and the capacitor bank was initially charged to 14.5 kV (representing 19.9 kJ of energy). The length of the exposed portion of wire was 102.5 mm, and the distance between the 32-AWG probe wires was 65.5 mm. Figure 24 contains a plot of the current data compared with results of a simulation where it was assumed that $R_p = 0$ mΩ. Agreement is good up to about the 6-μs point. In this case, the current rises noticeably after $t = 13$ μs, suggesting that some of the vapor is being converted to a more conductive plasma at that point.

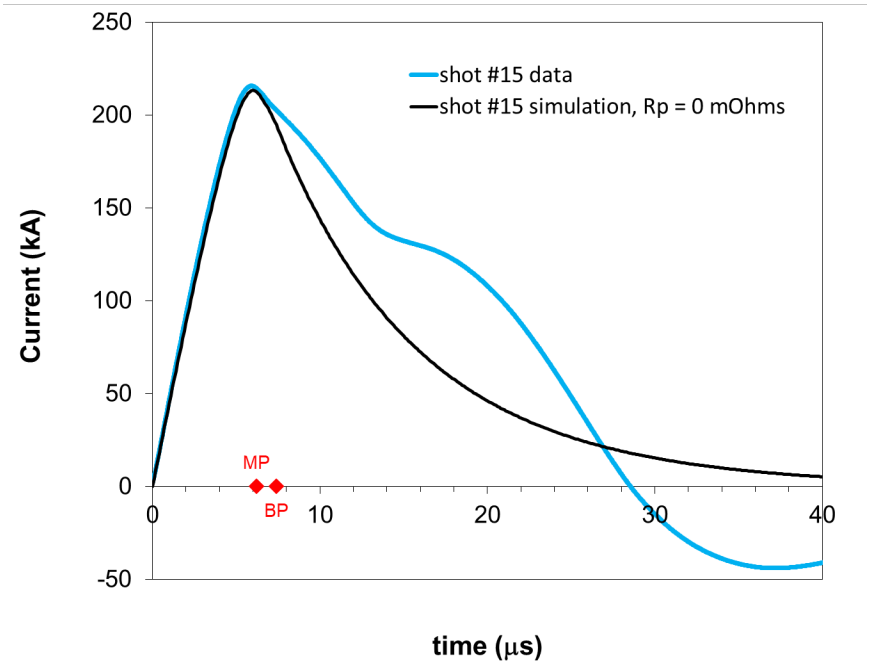

Fig. 24 Shot #15 current data compared with a simulation

Figure 25 contains plots of the voltage data obtained from Shot #15 compared with the results of simulations where it was assumed that $R_m = 0$ mΩ. Agreement is adequate in the short time that the model is valid. Once again, the W vapor seems to shift to a low-resistance mode quickly, and there is no clear sign of a "burst" peak in the data, though the shoulder at $t = 13$ μs may be the beginning of one.

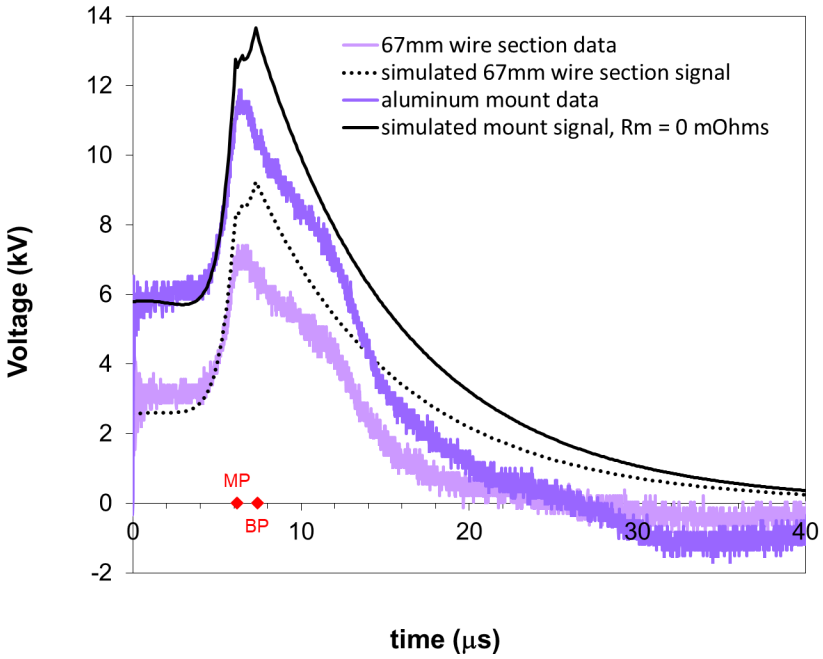

Fig. 25 Shot #15 voltage data compared with simulations

Figure 26 contains two high-speed video frames, the first taken at $t = 6.95$ μs, roughly corresponding to the when the melting point is reached in the simulation, and one taken at $t = 13.95$ μs, roughly when the resistance begins to drop. The latter image is overexposed, but it appears that the expansion was relatively uniform once again.

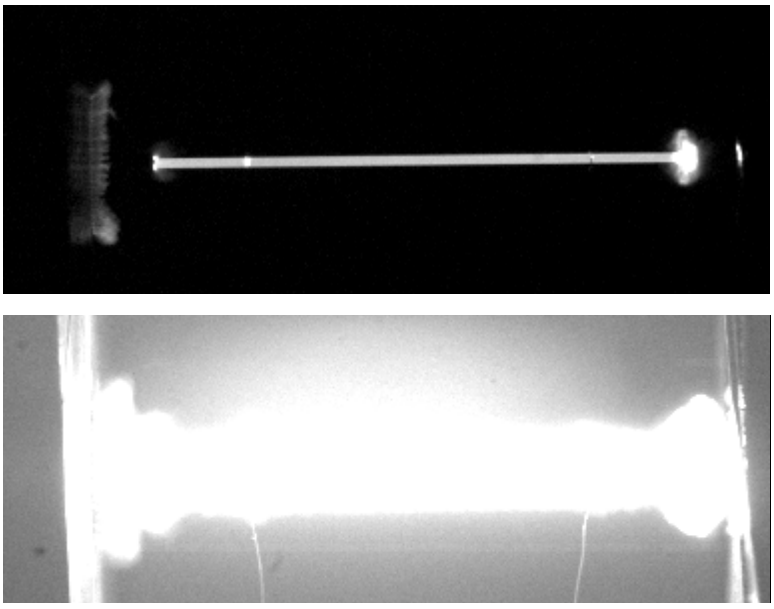

Fig. 26 Two high-speed video frames from Shot #15

"Shot #14" was an experiment in which a W wire was used, and the capacitor bank was initially charged to 18.0 kV (representing 30.6 kJ of energy). The length of the exposed portion of wire was 101.9 mm, and the distance between the 32-AWG probe wires was 66.8 mm. Figure 27 contains a plot of the current data compared with results of a simulation where it was assumed that $R_p = 0$ mΩ. Once again, agreement is good up to about the 6-μs point. In this case, the current recovery seen after $t \cong 10$ μs is much more pronounced than that seen in Shot #15. It is possible that the higher energies used in the W shots allows plasma to form almost immediately after vaporization. The dip in the curve around the $t =$ 10-μs mark resembles what occurs during "burst".

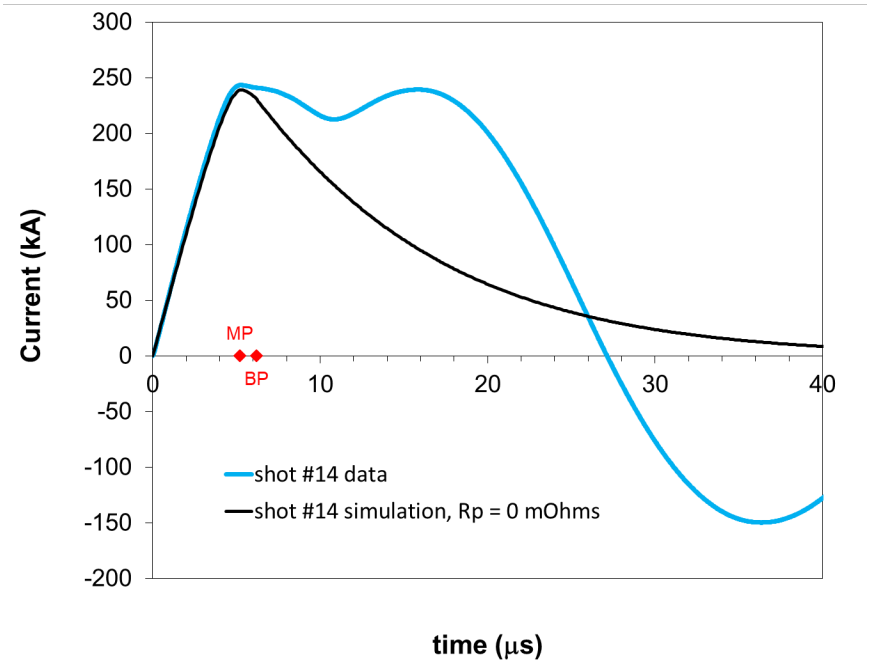

Fig. 27 Shot #14 current data compared with a simulation

Figure 28 contains plots of the voltage data obtained from Shot #14 compared with the results of simulations where it was assumed that $R_m = 0$ mΩ. The level of agreement is consistent with the previous W shots. There is no definitive sign of a "burst" peak; however, the structure around the $t = 10$-μs mark may be the beginning of one.

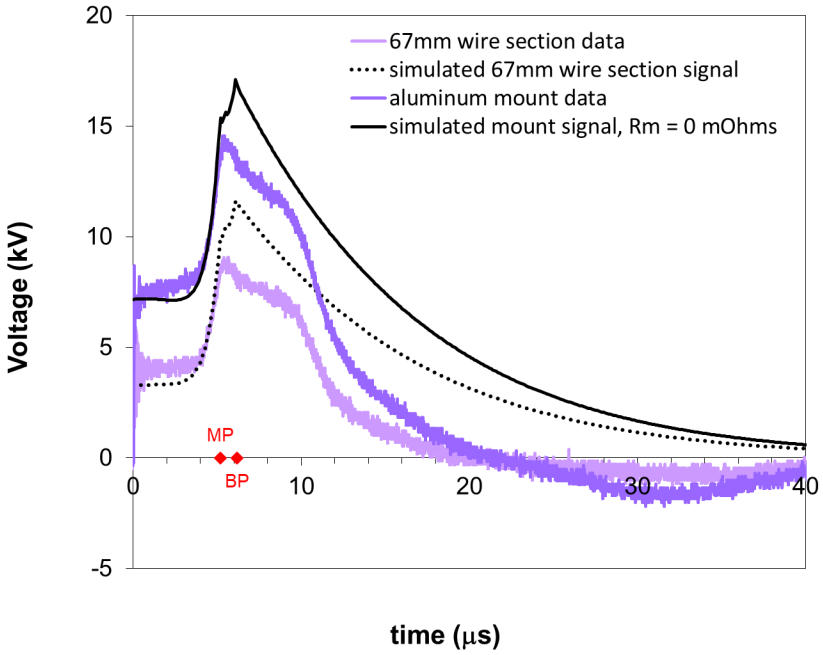

Fig. 28 Shot #14 voltage data compared with simulations

No high-speed video data were obtained in Shot #14.

3.4 Ti Wire Experiments

As the higher-energy experiments resulted in rapid vaporization and thus rapidly made the model irrelevant, it was decided to perform an unusually low-energy experiment with Ti such that the wire would not (in theory) ever reach the boiling point. In a case like this, the model should, in theory, remain valid throughout the entire pulse. In "Shot #20", a Ti wire was used and the capacitor bank was initially charged to a 4.5 kV (representing 1.9 kJ of energy). The length of the exposed portion of wire was 102.7 mm, and the distance between the 32-AWG probe wires was 65.6 mm.

Figure 29 contains a plot of the current data and the results of a simulation in which $R_p = 0$ mΩ. Unlike all the previous cases, the predicted pulse shape and peak current were in significant disagreement with the data. As can be seen in Fig. 29, simulations indicated that the parasitic resistance had to be set to an unprecedented 13 mΩ to match the measured peak current and pulse shape.

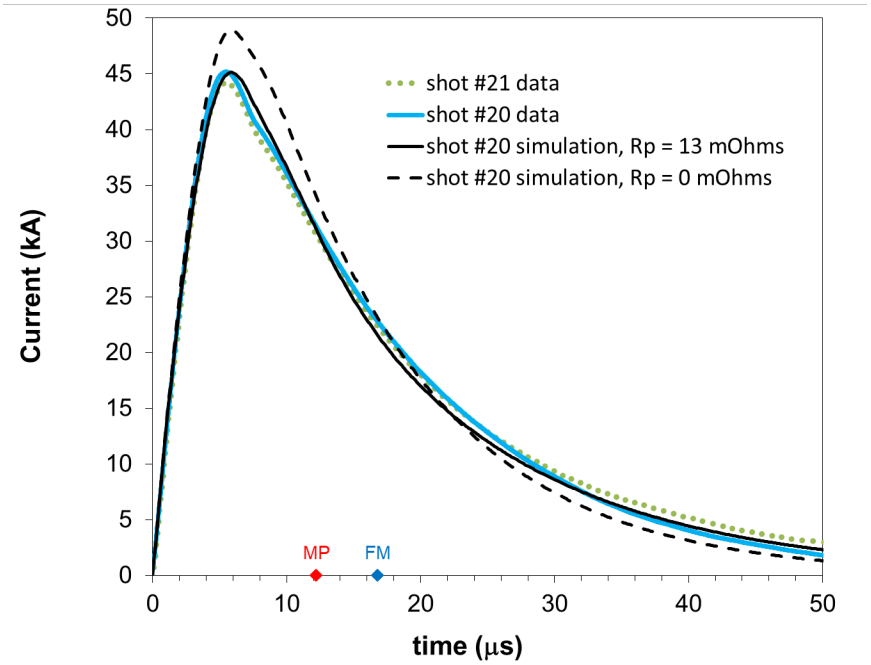

Fig. 29 Shots #20 and #21 current data compared with simulations

Since the boiling point is unachievable in this case, the point in time when the wire (theoretically) fully melts is marked in Fig. 29 instead ("FM").

It was hypothesized that loose connections between the metal parts and the graphite plugs may be responsible for this discrepancy, though some of the W cases had a slightly loose fit as well. With that in mind, an identical shot ("Shot #21") was performed where graphite "paint" (i.e., colloidal graphite particles suspended in isopropyl alcohol) was used to seal the joints between the graphite plugs, the Al wire mounts, and the Ti wire. Current data from Shot #21 are also plotted in in Fig. 29, where it can be seen that the effort had virtually no effect on the pulse shape (nor did it have a significant effect on the voltage data). As a testament to the quality of the bond between the graphite and the Al formed by the graphite paint, one of the graphite plugs could not be removed from the hole in its Al mounting block, even via chiseling, and the entire piece had to be discarded.

Figure 30 contains plots of the voltage data obtained from Shots #20 and #21 compared with the results of simulations where it was assumed that $R_m = 0$ mΩ (the Shot #21 data were smoothed to reduce the noise level). The predicted signal for the 66-mm wire section matched the data relatively well over the full length of the pulse. The predicted wire mount signal did not agree with the data quite as well, particularly in the tail region. As can be seen in Fig. 30, when the model assumes that $R_m = 11$ mΩ, that deficiency is repaired. The reason for this idiosyncrasy is unknown.

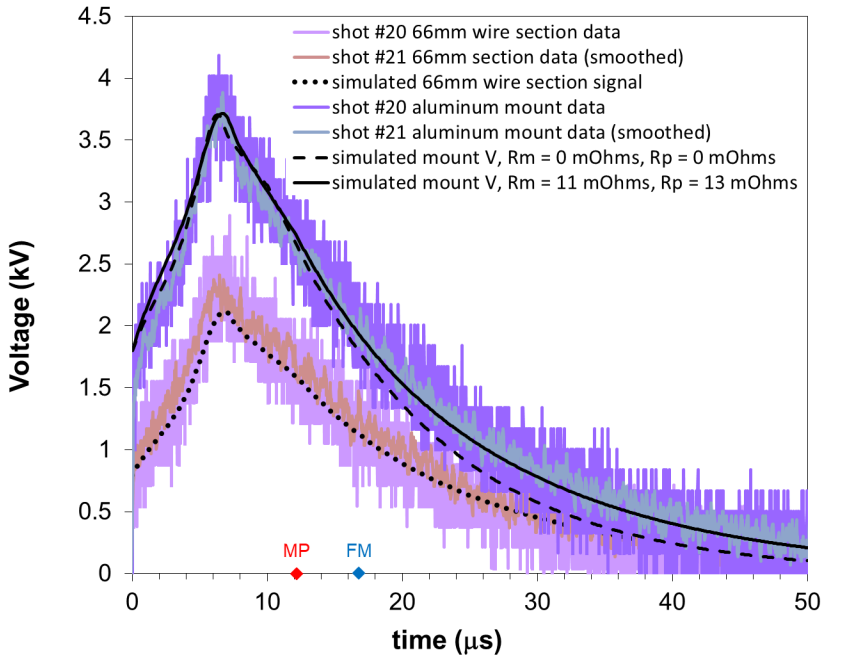

Fig. 30 Shots #20 and #21 voltage data compared with simulations

While high-speed video was recorded during Shot #20, the wire itself never got hot enough to be seen. All that was visible were jets of hot gas emanating from the graphite-to-wire joints. The ends of the wire remained intact. Figure 31 contains a high-speed video frame, taken at $t = 20.01$ μs, that shows the two clouds of hot gas spewing out of the joints. Since the chemical reactions between Ti and C, N, and O are all highly exothermic,[10,11] it is possible that arcs in these joints are driving those reactions and causing a localized increase in temperature at the Ti–C interface.

Fig. 31 High-speed video frame from Shot #20

"Shots #18 and #19" were nearly identical experiments in which a Ti wire was used, and the capacitor bank was initially charged to 7.0 kV (representing 4.6 kJ of energy). Shot #19 was performed because the high-speed video data in Shot #18 was lost. The length of the exposed portion of wire in Shot #18 was 101.8 mm, and the distance between the 32-AWG probe wires was 65.2 mm. In Shot #19, those numbers were 101.4 and 65.2 mm, respectively. Figure 32 contains plots of the

current data compared with results of simulations. Note that the two datasets virtually overlay each other. As can be seen in Fig. 32, assuming R_p = 0 mΩ leads to poor agreement; a parasitic resistance of R_p = 14 mΩ was required to match the peak current (much like Shots #20 and #21). Agreement beyond the peak is not as good as in Shots #20 and #21, but this is to be expected, as vaporization occurred in this case.

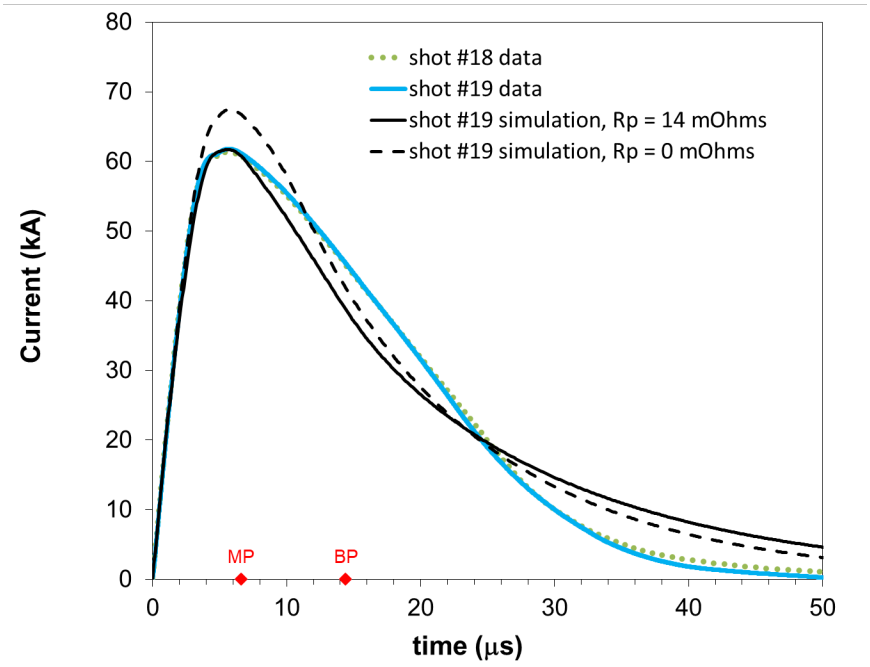

Fig. 32 Shots #18 and #19 current data compared with simulations

Figure 33 contains plots of the voltage data obtained from Shot #19 compared with the results of simulations. As can be seen, agreement is best when R_m = 10 mΩ, similar to what occurred in Shot #20. There is no sign of a "burst" peak in this data.

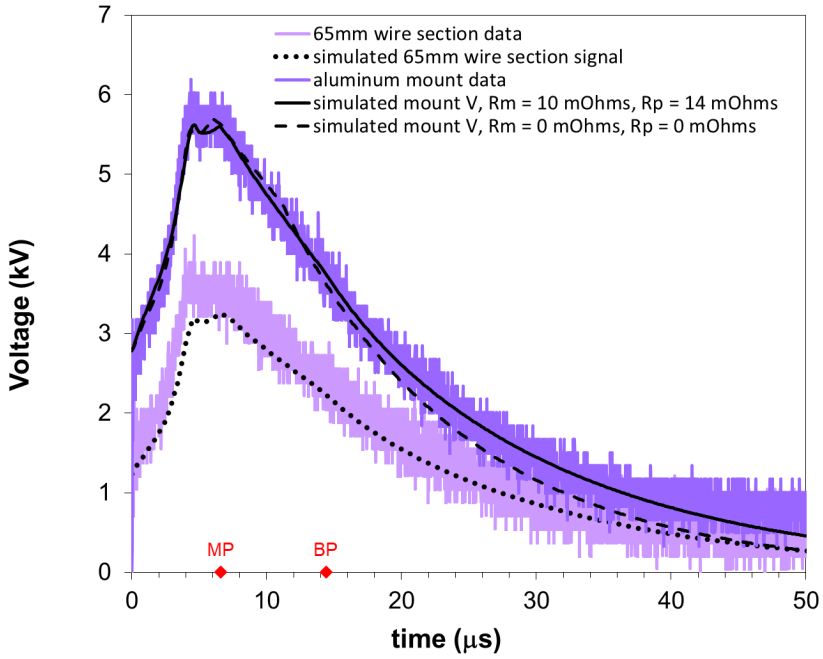

Fig. 33 Shot #19 voltage data compared with simulations

Figure 34 contains a high-speed video frame taken at $t = 29.82$ μs. It shows that aside from an instability near the right end, the wire expanded fairly uniformly. The larger clouds at the wire ends, which would normally be associated with instabilities, have an unusual shape. It is difficult to tell if hot gas emanating from the wire/graphite joint is contributing to them.

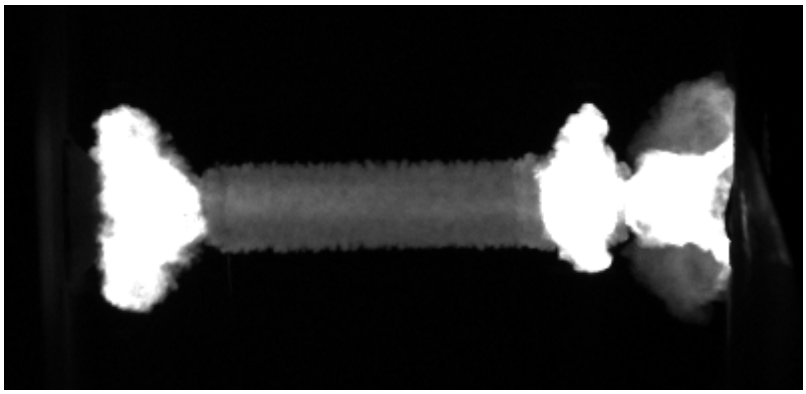

Fig. 34 High-speed video frame taken from Shot #19

"Shot #17" was an experiment in which a Ti wire was used, and the capacitor bank was initially charged to 9.5 kV (representing 8.5 kJ of stored energy). The length of the exposed portion of wire was 101.5 mm, and the distance between the 32-AWG probe wires was 64.5 mm. Figure 35 contains a plot of the current data compared with results of simulations. Once again, a large parasitic resistance (R_p = 14 mΩ) must be assumed to match leading edge (the exact value of R_p used

here is somewhat arbitrary, as the fit is poor). Beyond the peak, the data dips around the t = 15-μs mark and then resurges, similar to what happens when "burst" occurs.

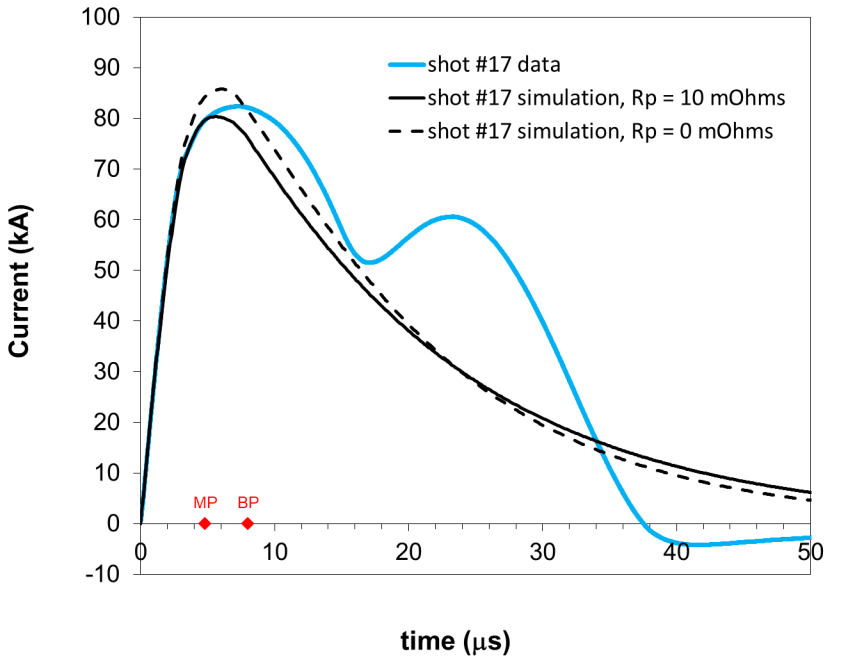

Fig. 35 Shot #17 current data compared with simulations

Figure 36 contains plots of the voltage data obtained from Shot #17 compared with the results of simulations. As can be seen, the low-temperature agreement is reasonable. As expected, a hint of a "burst" peak is visible near the t = 15-μs mark.

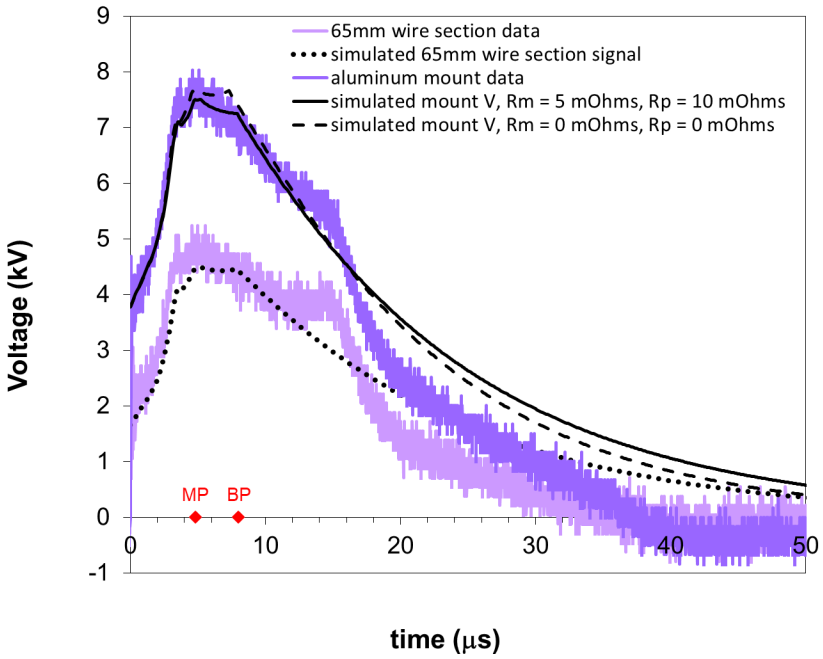

Fig. 36 Shot #17 voltage data compared with simulations

Figure 37 contains a high-speed video frames, taken at $t = 15.91$ μs, near where the "burst" peak occurs. Aside from likely instabilities at the ends, expansion seems quite uniform.

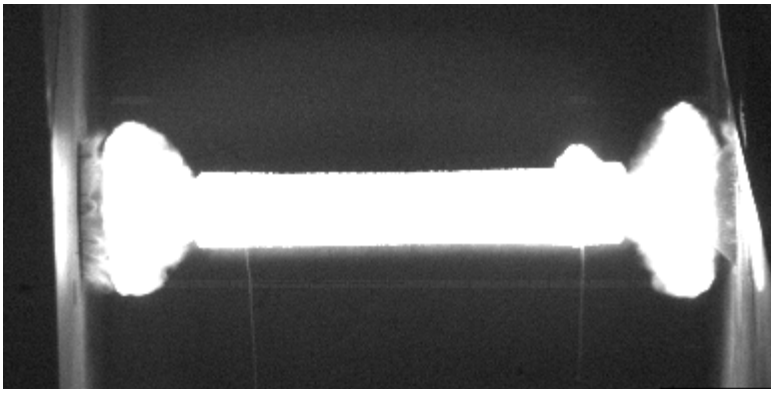

Fig. 37 High-speed video frame taken from Shot #17

4. Conclusion

A series of exploding-wire experiments was performed involving Cu, Al, W, and Ti wires. Current and voltage data were collected and compared with the results of simulations made using the exploding-wire circuit model described in Berning and Coppinger.[1] The model performed well up to when the boiling point was reached (an in some cases beyond that for a bit), but not well in the vapor phase, as it was not designed to handle that situation. The model worked particularly well in lower-

energy experiments and worked best in an experiment where the temperature of most of the wire never reached the boiling point. While the model overestimated the effects of phase changes on the voltage signals, it accurately predicted the timing of the phase changes.

The fidelity of the model proved insufficient to accurately measure small levels of parasitic resistance in the exploding-wire circuit, but it did successfully aid in characterizing the odd behavior seen in the Ti wire cases, where the wire mounting system suddenly acquired significant amounts of parasitic resistance.

Ultimately, the limited goals of the model development were met: The model successfully predicted key parameters such as the peak currents achieved and the timing of phase changes.

5. References

1. Berning PR, Coppinger MJ. An exploding wire circuit model. CCDC Army Research Laboratory; 2020 June. Report No.: ARL-TR-8983.

2. Robinson AC, Brunner T, Carroll S, Drake R, Garasi C, Gardiner T, Haill T, Hanshaw H, Hensinger D, Labreche D, et al. ALEGRA: an arbitrary Lagrangian–Eulerian multimaterial, multiphysics code. 46th AIAA Aerospace Science Meeting; 2008 Jan. AIAA Paper No.: 2008-1235. p. 1196–1235. https://doi.org/10.2514/6.2008-1235.

3. Doney RL III, Vunni GB, Niederhaus JH. Experiments and simulations of exploding aluminum wires: validation of ALEGRA-MHD. Army Research Laboratory (US); 2010 Sep. Report No.: ARL-TR-5299.

4. Zellner MB, Doney R III, Uhlig WC, Berning P, Bartkowski P, Halsey S. Concept for spatial visualization of magnetic fields from exploding wires. CCDC Army Research Laboratory; 2019 June. Report No.: ARL-TR-8706.

5. Berning PR, Bartkowski PT. A high-voltage capacitor bank design with a built-in spark gap switch. CCDC Army Research Laboratory; 2020 July. Report No.: ARL-TR-8995.

6. Coppinger MJ. CCDC Army Research Laboratory, private communication; 2020 Jan 10.

7. Vunni GB. Electrical exploding nickel and tungsten wires in air and water. Army Research Laboratory (US); 2009 Feb. Report No.: ARL-CR-619.

8. Gathers GR. Dynamic methods for investigating thermophysical properties of matter at very high temperatures and pressures. Rep Prog Phys. 1986;49:341–396.

9. Grover FW. Inductance calculations. Dover Publications; 2004.

10. Vrel DL, Lihrmann J-M, Petitet J-P, Synthesis of titanium carbide by self-propagating powder reactions. 1. Enthalpy of formation of TiC. J Chem Eng Data. 1995;40:280–282.

11. National Institute of Standards and Technology (NIST) database. https://webbook.nist.gov.

Appendix – Summary of Experimental Parameters

Table A-1 Parameters associated with 16 exploding-wire experiments

Shot #	Material	V_0 (kV)	E (kJ)	Length (mm)	Probe spacing (mm)	ΔV Data obtained	I_{max} (kA)	L_{tot} (nH)	f/ stop
5	Cu	7.5	5.32	101.29	65.53	Mount, wire center	171.1	314.4	2.8
6	Cu	10.0	9.45	101.64	64.12	Mount, wire center	229.2	312.8	8
7	Cu	12.5	14.77	101.64	65.18	Mount, wire center	285.1	305.9	16
8	Cu	10.0	9.45	…	…	Mount	226.5	312.3	8
9	Cu	10.0	9.45	…	…	Mount	228.8	311.8	8
10	Al	10.0	9.45	100.76	65.18	Mount, wire center	211.4	312.5	16
11	Al	8.0	6.05	100.06	65.53	Mount, wire center	175.2	314.0	16
12	Al	6.0	3.40	102.00	64.83	Mount, wire center	132.7	322.6	16
13	Cu	12.5	14.77	…	…	…	281.6	310.0	…
14	W	18.0	30.62	101.92	66.81	Mount, wire center	243.4	304.1	…
15	W	14.5	19.87	102.49	65.48	Mount, wire center	215.6	312.2	8
16	W	11.0	11.43	101.35	64.91	Mount, wire center	179.9	336.7	8
17	Ti	9.5	8.53	101.54	64.53	Mount, wire center	82.4	334.2	8
18	Ti	7.0	4.63	101.79	65.23	Mount, wire center	61.4	339.2	…
19	Ti	7.0	4.63	101.44	65.23	Mount, wire center	61.8	339.8	8
20	Ti	4.5	1.91	102.69	65.59	Mount, wire center	45.2	358.1	4
21	Ti	4.5	1.91	…	…	Mount, wire center	44.2	360.0	…

List of Symbols, Abbreviations, and Acronyms

Al	aluminum
AWG	American wire gauge
C	capacitance
Cu	copper
L	lumped inductance
MHD	magneto-hydrodynamic
R	lumped resistance
Ti	titanium
W	tungsten

1 (PDF) DEFENSE TECHNICAL INFORMATION CTR DTIC OCA

1 (PDF) DEVCOM ARL FCDD RLD DCI TECH LIB

20 (PDF) DEVCOM ARL FCDD RLW T R FRANCART FCDD RLW TA P BERNING WC UHLIG S BILYK J FLENIKEN T KOTTKE M MCNEIR C WOLFE M COPPINGER L VANDERHOEF A VALENZUELA B WILMER J NESTA D MALONE FCDD RLW TD B KRZEWINSKI A BARD R DONEY G VUNNI M ZELLNER FCDD RLW TE P SWOBODA